Peculiar adsorption induced by strong hydrogen bonds on perfect anatase (0 0 1) surface

Jialu Chen, Alexis Markovits, Ruiqin Zhang

Peculiar adsorption induced by strong hydrogen bonds on perfect anatase (001) surface

Jialu Chen,[1] Alexis Markovits*[2], Ruiqin Zhang*[1,3]

[1]Department of Physics, City University of Hong Kong, Hong Kong SAR, People's Republic of China

[2]Sorbonne Université, Laboratoire de Chimie Théorique, UMR 7616 CNRS, 75005 Paris, France

[3]Beijing Computational Science Research Center, Beijing 100193, People's Republic of China

*Corresponding author

Email address: alexis.markovits@sorbonne-universite.fr

aprqz@cityu.edu.hk

ABSTRACT

Titanium dioxide is a material with a wide range of applications in several fields, and understanding its interaction with molecules is fundamentally important for improvements of the various performance of materials. One important point not always sufficiently considered is the surface coverage of adsorbates on TiO_2 surfaces. In this work, we studied NH_3 adsorption at different coverages and cell sizes on the anatase (001) surface by means of density functional theory (DFT) calculations. The structural differences for given coverages of 0.25 at 1/4 and 4/16 ML are very significant depending on the cell size. Upon adsorption, there are Ti-O bond breaking, and enhanced hydrogen bondings between NH_3 and surface oxygen at only 4/16 ML coverage. The result shows that the use of a small cell cannot reproduce the surface relaxation due to the large displacement of underlying O atoms and surface Ti-O bonds breaking. Bond breaking and reformation of Ti-O bonds, and desorption of NH_3 have been observed in ab initio molecular dynamics simulations. Similar structural relaxation was also confirmed with H_2O and H_2S adsorption. It was revealed that the adsorptions are induced by the high reactivity of the anatase surface and hydrogen bonding with adsorbates. The strong hydrogen bonding effects causing chemical bond breaking challenge conventional surface chemical bonding mechanisms.

Keywords: ammonia; titanium dioxide; coverage; density functional theory; molecular dynamics

1. INTRODUCTION

Titanium dioxide (TiO_2) is a widely studied material because of its potential applications in several fields. TiO_2 exhibited excellent reactivity in heterogeneous catalysis [1-4] and photocatalysis [5-8]. Moreover, its special properties also make it possible to be used as pigment [9-12], gas sensors [13-16], and solar cells [17-20]. Studying the surface chemistry of TiO_2 is mandatory to improve its performance in these applications.

Actually, many crystal structures of TiO_2 have been found but are mainly in three forms in nature, namely rutile, anatase, and brookite. The anatase TiO_2

possesses higher catalysis than the rutile, the most stable crystal. While the most exposed surface of anatase TiO_2 is the (101) surface, both experimental results [21-24] and theoretical calculations [25, 26] show that the (001) surface is more reactive.

The adsorption of a very high number of molecules [26-34] including formic acid [35], proline [36], glycine [36], acetone [37], methanol [38], ethylene glycol [39], ammonia [17, 40-42], and water [43, 44] on TiO_2 surfaces have been studied by experiments or theories. However, the effects of coverage of adsorbates and the size of the cell used for modeling have been less explored.

Many factors, such as temperature, pressure, vacancies, or impurities, can affect the material's surface reactivity. A usually ignored important fact is the adsorbates coverage on the surface that can determine the reaction mechanism, as demonstrated with NO reduction on platinum surfaces [45]. The experimental and theoretical study of this electrocatalysis reaction found that the first hydrogenation product can be NHO or NOH, depending on the coverage. The final products are the same despite the different intermediates formed. Very recently, the photocatalysis mechanism of ethylene glycol on the rutile TiO_2(110) surface has also been experimentally found to be coverage dependent [39]. CH_2O and H are formed by C-C bond cleavage at low coverage, while CH_3CHO and H_2O are produced by C-O bond cleavage at high coverage. These observations show that coverage effects should be considered for material design.

Therefore, understanding the adsorption mechanisms, especially at different coverages, is fundamentally important for understanding the reactivities of TiO_2 surfaces. The interaction between NH_3 and TiO_2 is regarded as a classical model of Lewis acid-base interactions [40, 46]. In addition, NH_3 could be one effective method to reduce NO_x on the surface [47, 48]. Studies of interaction mechanisms on anatase surfaces taking into account coverage and cell size are still insufficient. The adsorption energy of NH_3 drops to 58 kJ mol^{-1} from 100 kJ mol^{-1} when the coverage increases to 1 ML from 0.5 ML on a rutile (011) surface [42]. Moreover, the adsorption energy on a brookite (100) surface is significantly lower than on a rutile (011) surface, and a linear dependence with the coverage has been found [41]. Thanks to the prototypical properties of NH_3 and reactivity of anatase (001) surface, the study of their interactions would be very helpful for understanding the surface chemistry

and catalysis processes of TiO_2.

In this work, we conducted a systematic study of NH_3 adsorption on the anatase (001) surface by performing density functional theory (DFT) calculations and molecular dynamic (MD) simulations. Different cell sizes and coverages were considered for exploring coverage effects. Interestingly, peculiar adsorption of NH_3, H_2O, and H_2S molecules with surface Ti-O bonds breaking was found on the anatase (001) surface at higher coverage. Indeed, we find that the hydrogen bond type under scrutiny is stronger than the surface Ti-O chemical bond. Very recently, a short strong hydrogen bond of $[F\text{-}H\text{-}F]^-$ ion observed by experiments [49] becomes comparable to covalent bonds. Based on theoretical results, it appears that the bond is a hybrid covalent-hydrogen bond rather than a simple hydrogen or covalent bond. Existence of this bond challenges the current understanding of chemical bonding [50]. Similar to the recent finding of $[F\text{-}H\text{-}F]^-$ ion, we found that a strong hydrogen bond makes surface chemical bonds break. It challenges the typical understanding of chemical bonds, which are much stronger than conventional hydrogen bonds. Our predictions call for experimental verifications, and we expect a better understanding of chemical bonds to be achieved in the future.

2. METHOD

Periodic DFT calculations were performed with the Vienna Ab Initio Simulation Package (VASP) [51-53] with the projector augmented wave method [54]. Perdew-Burke-Ernzerhof (PBE) exchange-correction functional [55] with DFT-D3 dispersion correction [56] has been used. An energy cutoff of plane-wave expansion of electron wavefunctions was set to be 400 eV. The U value of the Hubbard model was chosen to be 3.5 eV for the Ti element to describe the strongly correlated interaction effects. There are 12 atoms per primitive cell, and supercells have been constructed to consider the effects of coverage and cell size. Half of the atoms are fixed to their bulk position. A vacuum layer of 15 Å with dipole correction [57] has been used in our calculations to avoid the interaction of one slab and its image by translation. The calculations were performed by sampling the Brillouin zone in $6 \times 6 \times 1$, $3 \times 3 \times 1$, $2 \times 2 \times 1$, and $1 \times 1 \times 1$ Monkhorst-Pack sets for 1×1, 2×2, 3×3, and 4×4 cells, respectively.

The average adsorption energy of NH_3 is calculated by the following equation:

$$E_{ad} = \frac{1}{n}(E_{gas/surf} - n * E_{gas} - E_{surf}) \quad (1)$$

where $E_{gas/surf}$ is the total energy of adsorbed molecules and the covered surface, and E_{gas} denotes the energy of a molecule in gas. In addition, E_{surf} equals the energy of the slab with a clean surface, and n is the number of adsorbed molecules.

In this work, ab initio molecular dynamics simulations were performed with VASP using a timestep of 0.5 fs and simulation time up to 3 ps. The Nosé–Hoover thermostat [58, 59] was used to control the temperature. The NVT ensemble with simulation temperatures of 300 and 400 K was chosen to understand the behaviors in a real environment. The optimized coordinates were selected as the initial structures. In addition, the initial velocities of atoms were sampled by Maxwell-Boltzmann distribution.

3. RESULTS AND DISCUSSION

3.1 Coverage and cell size

As shown in Figures 1a and 1b, NH_3 molecules interact by N with the surface Ti atom at 1/1 ML (one NH_3 per 1 × 1 cell) and 1/4 ML (one NH_3 per 2 × 2 cell) coverage. The N-Ti bond is not perpendicular to the surface due to the interaction between the surface O atom and the H atom of NH_3. No distinctive changes of the surface structure have been observed, similarly to calculations of NH_3 chemisorption on the brookite (100) surface [41]. However, significant differences of structures at lower coverages (1/9 ML, 1/16 ML) surfaces have been found (Figures 1c and 1d). One O atom rises from the surface, causing one Ti-O bond breaking, and the length of the hydrogen bond becomes shorter by ~0.2 Å.

Moreover, the detachment of the O atom also yields the deviation of other surface atoms. In order to distinguish this special adsorption from general chemisorption, we call adsorption with bond breaking “cleavage” and general adsorption “chemisorption”. The adsorption of NH_3 is cleavage at low coverage instead of chemisorption at high coverage. This kind of significant surface structure changes controlled by the coverage has seldom been reported before [43, 44, 60]. To

pursue our calculations, we expand the adsorption structures of 1/1 ML to a 4 × 4 supercell with 16 NH_3 molecules per cell, referred to as 4/4 ML keeping the coverage constant. This structure, 16/16 ML, was optimized (Figure 1f), and a similar structure to 1/1 ML (Figure 1a) was obtained, showing chemisorption. Interestingly, decreasing the coverage to 1/4 ML and keeping the same supercell (4 NH_3 per 4 × 4 supercell), 4/16 ML, the optimized structure is the combination of chemisorption and cleavage, different from chemisorption at 1/4 ML coverage in Figure 1b. The staggered arrangement of cleavage and chemisorption is shown at this coverage in Figure 1e. The discrepancies of these results between a small cell and a larger cell mention that using a small slab to reduce the computational costs may cause inaccurate descriptions of the surface structures.

In Figures 1g-j, two different configurations at 8/16 ML coverage were also optimized. One yields Ti-O bond breaking while the other does not. These results show that for a given cell size and a given coverage, the relative arrangement of the adsorbates significantly affects the surface structure and adsorption mode.

The adsorption mode is found to depend on adsorbate-adsorbate interaction, like CO_2 adsorption on TiO_2 [61]. Interestingly, ammonia can adsorb with completely different structures at the same coverage depending on the cell size and its relative position. These results demonstrate that various configurations are stable at the same coverage and that the most stable one may be very complicated. It is also shown that the adsorbate arrangement for a given cell size and a given coverage has to be carefully studied. Surface Ti-O bond breaking is obtained for one arrangement and not for another one.

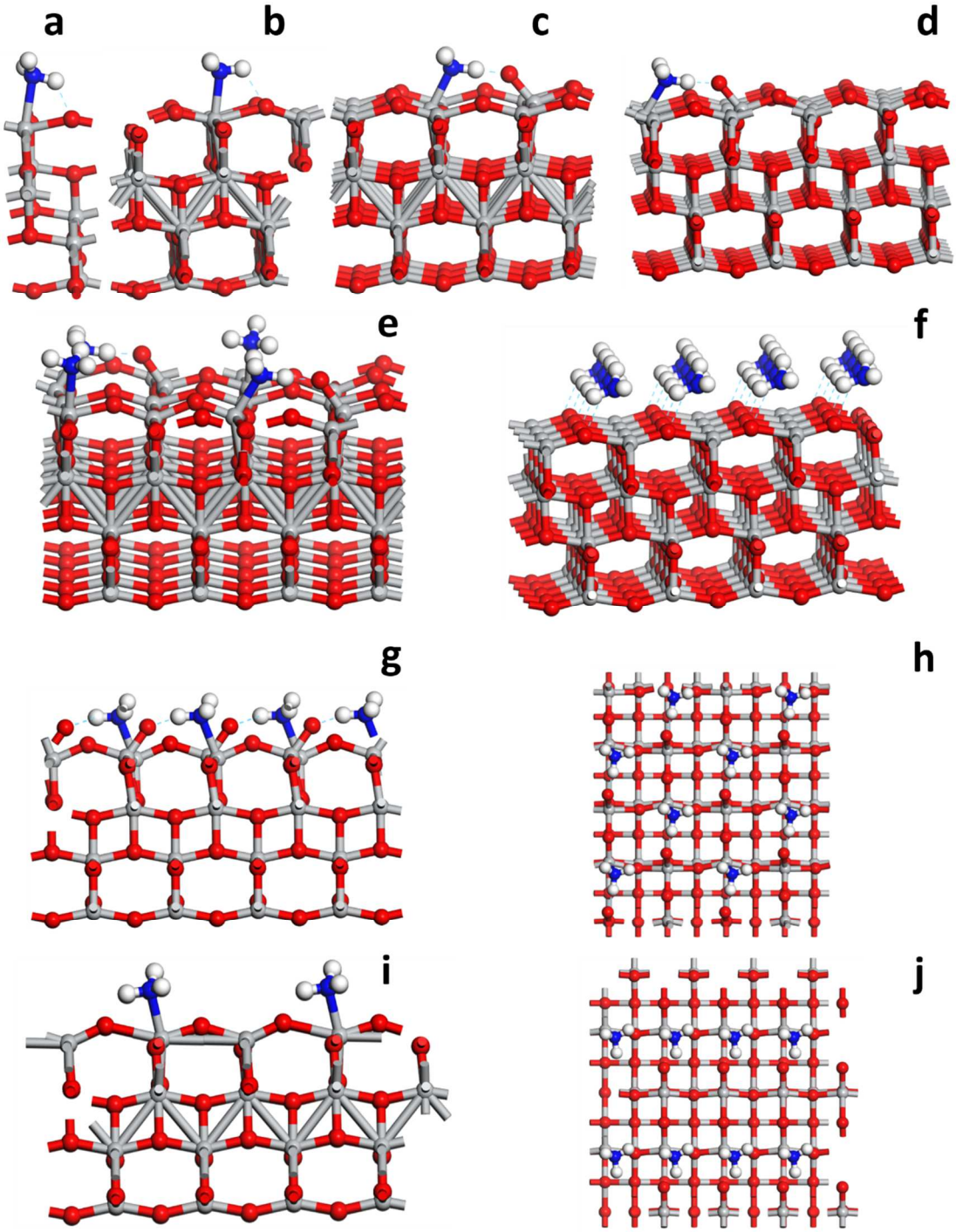

Figure 1. The optimized structures at 1/1 ML (a), 1/4 ML (b), 1/9 ML (c), 1/16 ML (d), 4/16 ML (e), 16/16 ML (f), side (g) and top (h) view of cleaved 8/16 ML, and the side (i) and top (j) view of chemisorbed 8/16 ML.

3.2 Energetics

In Table 1, we compare our adsorption energies with previous calculations and experiments. The adsorption energy at 4/16 ML coverage is in good agreement with

experiments [62]. The previous calculations of Onal [63] are also close to our results at 1/4 ML coverage since both calculations were performed on the 2 × 2 cell. The unprecedented increase of adsorption energy from -2.77 to -0.83 eV demonstrates the great importance of the surface structure. The interaction strength at coverage 1/4 ML is -1.28 eV. It becomes -2.14 eV at 1/9 ML. This large difference cannot be explained only by the drop of lateral repulsion between adjacent adsorbates, especially since there is a surface Ti-O bond breaking at 1/9 ML. We must invoke the unusually strong hydrogen bond allowed by the Ti-O bond breaking. The adsorption energy at 4/16 ML is close to the average value of 1/16 and 16/16 ML owing to its mixed surface structure. It is also lower than at 1/4 ML showing the stabilization allowed by surface reorganization only when the size of the cell is large enough.

The gap of adsorption energies is only -0.25 eV between our two systems at 8/16 ML coverage, much smaller than the gap between the energies at coverage 1/4 ML and 1/9 ML. Even if lateral repulsions have to be considered at high coverage, it is not the only point. Our results show that high coverage also limits surface relaxation. At 8/16 ML, for instance, there could be eight Ti-O bonds breaking. Therefore, the gap between cleavage and chemisorption becomes much smaller owing to insufficient surface relaxation for such bond breaking. In Figure 2, the trend of adsorption energies with increasing coverage is presented. The interaction strength drops sharply with coverage, and it can be fitted by an exponential function.

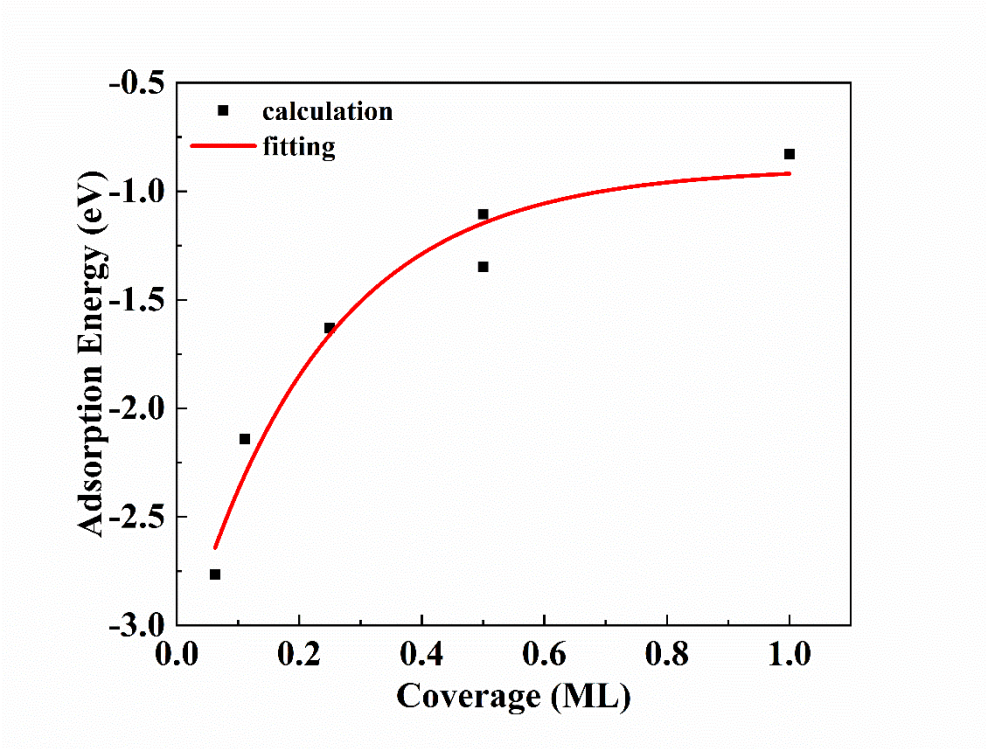

Figure 2. The adsorption energy of NH_3 at different coverage and its fitting curve with an exponential function.

3.3 Geometry

In Table 2, we list the length of the N-Ti bond, four Ti-O bonds, and the hydrogen bond. Each Ti atom connects with four O atoms in two layers. As shown in Figure 3, the two uppermost O atoms are denoted as O1 or O2, and the hydrogen bond involved one is O1. The length of the Ti-N bond in the case of cleavage is 0.1 Å shorter than chemisorption. The length of the Ti-N bond at 1 ML coverage (chemisorption) is 0.15 Å longer than at 1/4 ML coverage in agreement with a stronger interaction. Let us compare the Ti-N bond length in the case of cleavage with the one in the case of chemisorption. This can be done by considering the two adsorption modes for a given coverage. It is easy to understand that breaking one Ti-O bond enhances interaction strength between N and Ti atoms since Ti lacks one neighbor. For both adsorption types, the length of Ti-O1 increases, and Ti-O2 decreases compared to the pure surface with four equal lengths of Ti-O bonds around 1.985 Å. The formation of the hydrogen bonds causes the tilt of NH_3, and thus squeezes the Ti atom to another side. The lengths of Ti-O3 and Ti-O4 almost keep constant during the chemisorption and cleavage process, which shows the down layers

of O atoms are not involved in the NH_3 adsorption. It is worth mentioning that the squeeze of Ti atoms is weakened, and hydrogen bonds are slightly shorter at 1/1 ML coverage, compared with chemisorption at 1/4 ML coverage. The repulsion of adsorbates hinders NH_3 molecules tilting and facilitates them to reorientate with enhanced hydrogen bonds interactions to decrease the repulsion. The difference of bond length of Ti-O1 between cleavage and chemisorption at 8/16 ML is smaller than at 4/16 ML. As a result, adsorption energies of weakened cleavage and enhanced chemisorption are very close, in the case of two 8/16 ML coverages.

Table 1. The comparison of adsorption energy (eV) between our results and previous calculations and experiments.

References	Method	Model	Adsorption Energy
Onal 2006 [64]	B3LYP/6-31G**	Relaxed cluster	-0.992
Erdogan 2009 [65]	B3LYP/6-31G**	ONIOM cluster	-0.845
Onal 2010 [63]	PW91	Periodic, 1/4 ML	-0.919
Roman 1991 [66]	TDS		-0.702
Srnak 1992 [67]	TPD		-0.61, -1.17
Sprinceana 1999 [62]	XRD BET		-1.34~-1.56
This work	PBE-D3+U	1/1 ML	-0.848
This work	PBE-D3+U	1/4 ML	-1.284
This work	PBE-D3+U	1/9 ML	-2.142
This work	PBE-D3+U	1/16 ML	-2.766
This work	PBE-D3+U	4/16 ML	-1.631
This work	PBE-D3+U	8/16 ML (cleavage)	-1.349
This work	PBE-D3+U	8/16 ML (chem.)	-1.105
This work	PBE-D3+U	16/16 ML	-0.830

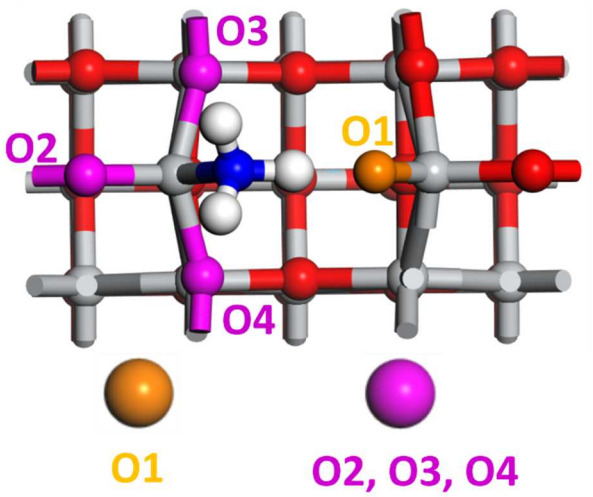

Figure 3. Atoms labels in the case of cleavage adsorption mode. Purple, orange, and red spheres represent oxygen atoms, while white and gray spheres correspondingly represent H and Ti atoms.

Table 2. The bond length (Å) and adsorption energy E_{ad} (eV) at different coverages. NH_3 molecules with different types of adsorption are discussed, respectively. The cleavage and chemisorption modes are listed respectively in the case of the mixed mode at 4/16 ML.

Coverage/ML	R(H-O1)	R(Ti-N)	R(Ti-O1)	R(Ti-O2)	R(Ti-O3)	R(Ti-O4)	E_{ad}
1/1	1.861	2.409	2.147	1.834	1.984	1.980	-0.848
1/4	2.045	2.242	2.415	1.824	1.985	1.985	-1.284
1/9	1.540	2.147	3.923	1.806	1.964	1.960	-2.142
1/16	1.587	2.161	4.125	1.810	1.969	1.964	-2.766
4/16 cleavage	1.539	2.154	4.055	1.806	1.967	1.967	-1.631
4/16 chem.	2.520	2.287	1.996	1.860	2.036	1.993	-1.631
8/16 cleavage	1.585	2.172	3.620	1.791	1.965	1.952	-1.349
8/16 chem.	1.885	2.267	2.521	1.818	2.061	1.990	-1.105
16/16	1.861	2.409	2.144	1.836	1.981	1.983	-0.830

3.4 Electronic structure

We performed Bader charge analysis, and the results are shown in Table 3. The charges of H atoms are around 0.5. In the cleavage case, O lost some negative charges. It is surprising since the hydrogen bond is stronger when Ti-O bond breaking occurs.

This is another proof that this kind of hydrogen bond is special. The charge of this O atom of Ti-O bond breaking is around -0.1 smaller than the average value. By contrast, the charges of Ti atoms of N-Ti bonds are close to the average value of surface Ti atoms, so the charges of Ti atoms are slightly affected by adsorption.

Table 3. The Bader charge at different coverage. The charges are averaged if there are more than one adsorbed NH_3 per unit cell. The charges averaged on total H, Ti and O atoms are also shown.

Coverage/ML	N	O1	Ti	Average H	Average Ti	Average O
1/1	-1.440	-1.028	2.021	0.495	2.019	-1.015
1/4	-1.310	-0.997	1.992	0.485	2.011	-1.010
1/9	-1.259	-0.895	1.981	0.473	2.010	-1.007
1/16	-1.293	-0.886	1.983	0.483	2.013	-1.008
4/16 cleavage	-1.306	-0.930	1.979	0.476	2.012	-1.010
4/16 chem.	-1.271	-0.995	2.021	0.476	2.012	-1.010
8/16 cleavage	-1.368	-0.994	1.967	0.508	2.007	-1.013
8/16 chem.	-1.323	-1.006	1.984	0.475	2.009	-1.011
16/16	-1.448	-0.999	1.983	0.498	2.013	-1.013

We have also calculated the total density of states (DOS) (Figure 4). They are slightly affected by NH_3 adsorption. The energy gap becomes larger with the increase of coverage. The upper limit of energy is not always increasing with coverage, and the largest one is at 8/16 ML coverage. At low coverage, 1/16 and 4/16 ML, the DOS is very similar, so the electronic structure of the surface is not influenced significantly. By contrast, the DOS is also similar at higher coverage but different from 1/16 and 4/16 ML coverage. Although the adsorbed structure is completely different for cleavage and chemisorption at 8/16 ML, their DOS is very similar. Therefore, the smallness of adsorption energies difference can be understood. The projected density of states (PDOS) is presented in Figure 5 to study the bond formation and orbital hybridization. The N-H bonding is extremely strong, with a considerable overlap from -4 to -3 eV and -1.5 to -0.5 eV. Overlap of N and Ti atoms, H and O atoms in many regions of PDOS demonstrates the strong interaction of N-Ti and hydrogen bonds.

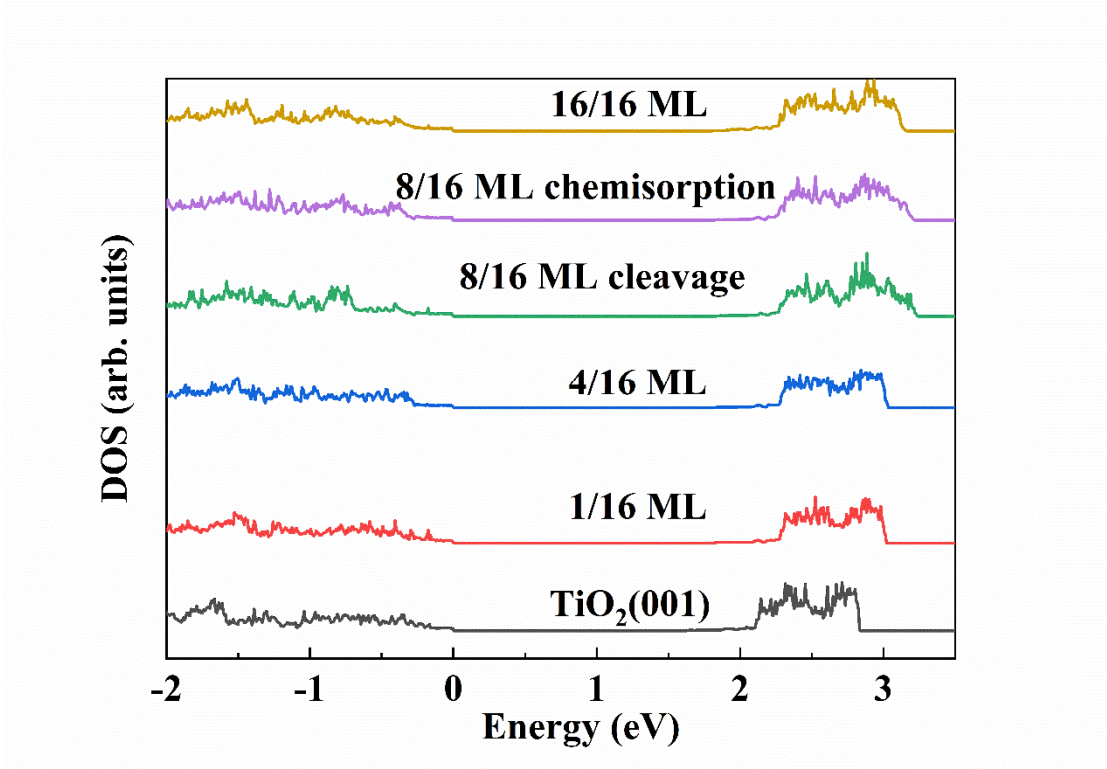

Figure 4. The density of states (DOS) of bare TiO_2 (001) surface and at different NH_3 coverages.

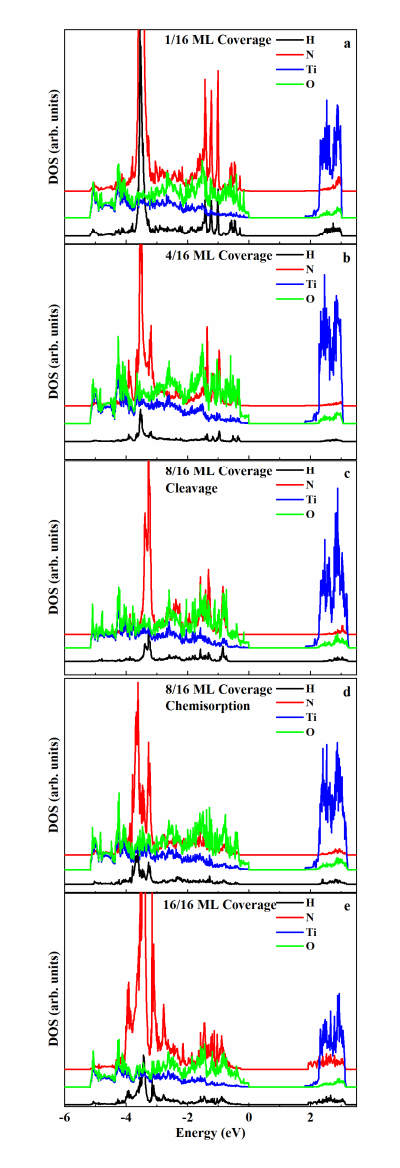

Figure 5. Projected density of states (PDOS) of 1/16 (a), 4/16 (b), 8/16 (c, d) and 16/16 (e) coverages.

3.5 Molecular Dynamics

As shown in Figure S1, we performed molecular dynamics at 1/9 and 1/16 ML coverage at 300 K. We did not observe surface Ti-O bonds reformation. MD results demonstrate the Ti-O bond breaking is stable at these low coverages due to significant surface relaxation with only one Ti-O bond breaking. In Figure 6, the snapshots and notable changes at 4/16 ML at 300 K can be seen. The O2 atom is very active so that a new Ti-O bond breaking can be clearly found in snapshots since 1 ps, and one hydrogen transfers from NH_3 to O in 2 and 3 ps. Actually, there is another Ti-O bond breaking and recombination in a short period, which cannot be seen in snapshots. In

order to have a quantitative insight, notable bond lengths are also presented in Figure 6. One Ti-O bond is broken after 0.5 ps and keeps this state, while another Ti-O bond is broken in 1 ps and recombines in 1.5 ps. In addition, based on the changes of N-H and O-H bond length, one hydrogen moves back and forth between N and O. It demonstrates a strong hydrogen bond effect because hydrogen transfer between O • • • H-N and O-H • • • N happens easily. However, the bond breaking and recombination, and hydrogen transfer are not found at 400 K by molecular dynamics at the same coverage. The snapshots at 400 K can be seen in Figure S2. The reason is that higher temperature makes the O atoms more active and hydrogen bonds weaker. Therefore, the O-Ti bond is always broken, and no recombination occurs and the hydrogen transfer becomes difficult owing to a higher free energy barrier.

The number of breaking Ti-O bonds is counted in Figure 7. The criterion is the bond length of Ti-O beyond 3 Å. In Figure 7a, the number of Ti-O bonds breaking increases more slowly at 400 K, and the final number is four instead of three. In Figure 7b, cleavage with eight Ti-O broken bonds and chemisorption with no broken bond have been compared. The number of broken Ti-O bonds decreases for cleavage and increases for chemisorption very quickly.

Interestingly, the final number is four for both initial configurations at 300 and 400 K. The snapshots can be seen in Figures S3 and S4. We also found one NH_3 desorption in chemisorption configuration at 300 K. Similar to counting the Ti-O bonds breaking, a Ti-N bond longer than 3 Å is regarded as desorption. At 16/16 ML coverage, the Ti-O bonds breaking and NH_3 desorption can be observed in Figure S5. Therefore, the structure with sixteen NH_3 molecules adsorbed is not stable. In Figure 7c, the final amounts of Ti-O bonds breaking and desorbed NH_3 molecules are sensitive to temperature at 16/16 ML coverage. By contrast, four Ti-O bonds are broken in 3 ps at 8/16 ML coverage, regardless of initial configurations (cleavage or chemisorption) and temperatures (300 or 400 K). NH_3 molecules are more likely to desorb at high temperatures, and thus fewer NH_3 molecules adsorbed on the surface facilitate surface relaxation yielding more Ti-O bonds breaking. Based on MD results, chemisorbed and cleaved NH_3 molecules convert spontaneously, so the chemisorption and cleavage mixture is more stable. The peculiar NH_3 adsorption with broken Ti-O bonds is expected to exist at any coverage.

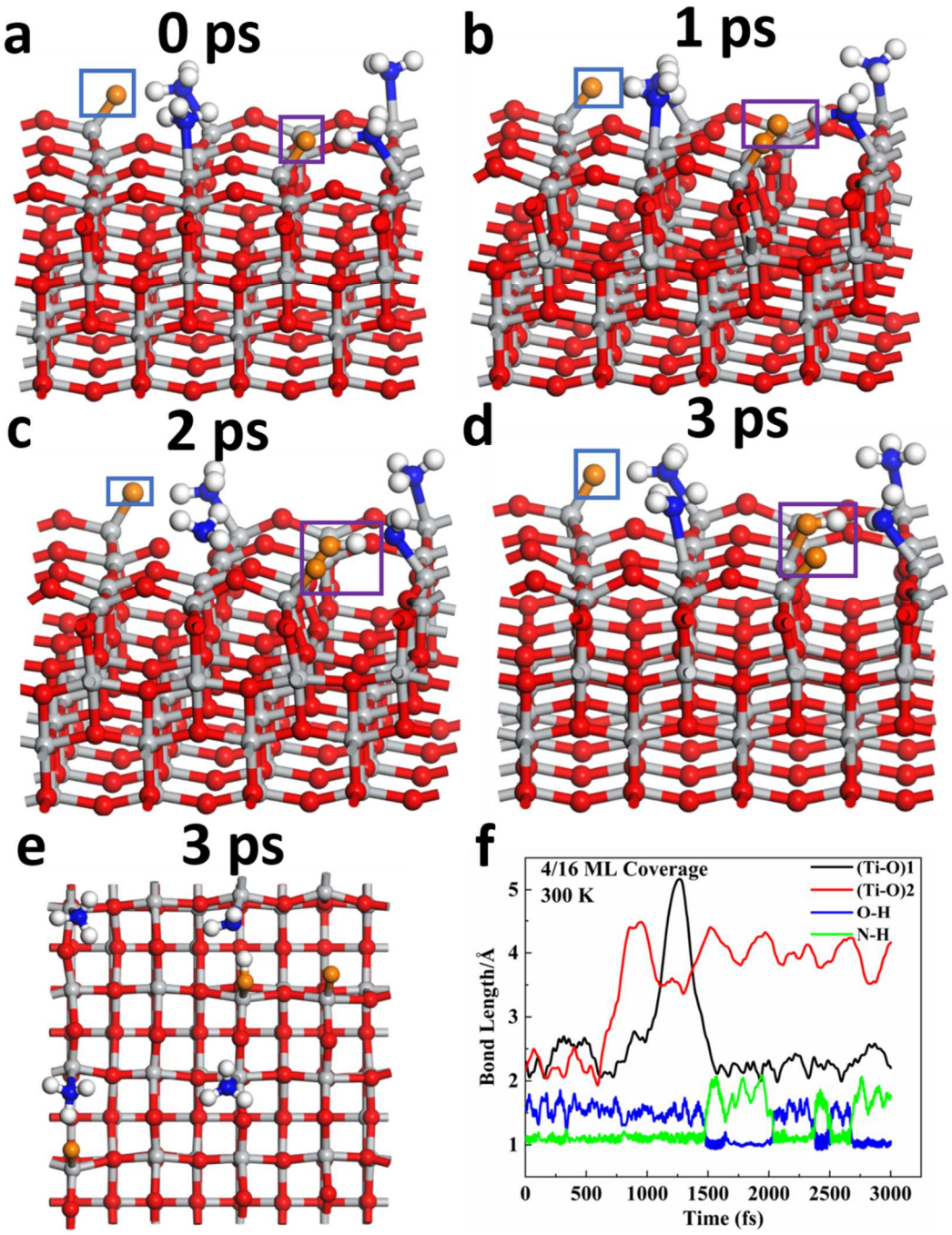

Figure 6. Snapshots of molecular dynamics simulations in 0 (a), 1 (b), 2 (c), and 3 ps (d, e) at 4/16 ML coverage, and notable changes of bond length (f) at 300 K. Orange and red spheres represent oxygen atoms. In contrast, white and gray spheres represent H and Ti atoms, correspondingly.

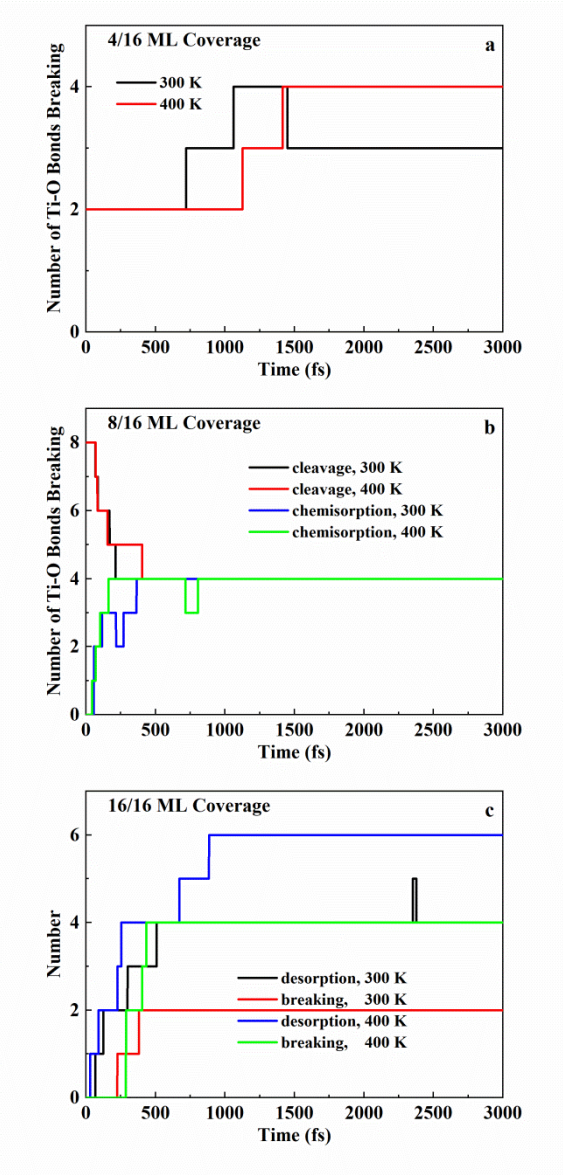

Figure 7. The number of Ti-O bonds breaking and NH_3 desorbed molecules at 4/16, 8/16, and 16/16 ML coverages.

3.6 H_2S and H_2O adsorption

The water molecules may have similar chemical properties as NH_3 on TiO_2 surfaces. Indeed, it can interact as a base through N with the surface acidic Ti. Yet, the large surface reorganization has not been observed for H_2O adsorption on TiO_2/SnO_2 rutile (110) surface at 1/12 and 1 ML coverage [68]. Moreover, H_2O adsorption at 0.25, 0.50, 0.75, and 1.0 ML coverage has been studied on several TiO_2

surfaces, including the anatase (001) surface [69]. No special adsorption structures have been mentioned. Interestingly, the peculiar adsorption properties on the same surface have been found in calculations with a larger cell and with the dissociative adsorption mode [44]. The computed adsorption energies change dramatically with the coverage, which is not simply induced by adsorbate-adsorbate repulsion nor any typical lateral interaction. This extraordinary behavior has never been observed on other surfaces. Since water molecules on the anatase (001) surface are also found to adsorb with bond breaking [44], the properties of water and ammonia are similar, and their adsorption mechanisms on the same surface are likely to be the same. The aforementioned NH_3 adsorption on the brookite (100) surface [41] has not been found to own properties like the anatase (001) surface. Therefore, the extraordinary adsorption characteristics may originate from the structure of the anatase (001) surface and the hydrogen bond interactions between adsorbates and surface O. In order to validate our conjectures, we also performed DFT calculations of H_2O and H_2S adsorption.

In Figure 8, the structures of H_2S and H_2O at different coverages are shown. Similar to NH_3, the H_2S adsorption has not caused the Ti-O bond breaking at 1/4 ML coverage. Nevertheless, the difference is that H_2S tends to dissociate directly at 1/16 ML coverage. We conclude that H_2S is more reactive than NH_3 on this surface. The adsorption of H_2O is different from NH_3 and H_2S adsorption, and it tends to dissociate at the three coverages. The surface relaxation with Ti-O bond breaking can even be observed at 1/4 ML coverage. The adsorbate dissociates into proton and anion, just like H_2O dissociates to OH^- and H^+ on the surface. The difference between these three molecules can be simply explained by the basicity of dissociative anion and surface oxygens, as proton tends to bind with a stronger base [70]. Dissociative adsorption of water molecules can be explained because the surface oxygen is a stronger base than OH^-. As a result, OH^- is less reactive and cannot attract a proton adsorbed on surface oxygens to reform a water molecule. By contrast, NH_2^- being a stronger base than surface oxygens explains the molecular adsorption. In addition, the HS^- basicity is comparable to the basicity of surface oxygens so molecular or dissociative adsorption of H_2S is determined by coverage. These DFT calculations proved our assumption that the strong hydrogen bond interactions between adsorbates and surface O are required to break Ti-O bonds on the anatase (001) surface.

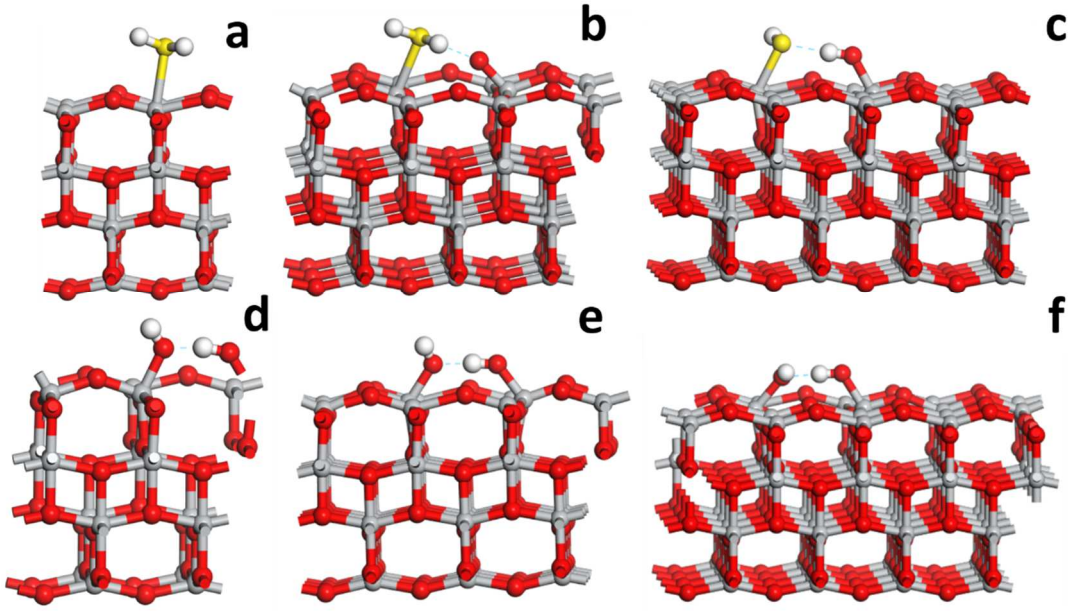

Figure 8. Optimized structures of H_2S at1/4 (a), 1/9 (b) and 1/16 (c) ML coverage, and H_2O at 1/4 (d), 1/9 (e) and 1/16 (f) ML coverage. White, gray, red, and yellow spheres represent H, Ti, O, and S atoms, correspondingly.

4. CONCLUSION

In conclusion, our DFT calculations revealed coverage-dependent mechanisms of ammonia adsorption on the anatase (001) surface. The large displacement of underlying O atoms and surface Ti-O bonds breaking affects adsorption energies significantly. Similar structure relaxation is also found for H_2O and H_2S adsorption. These peculiar adsorption mechanisms are induced by specific reactivity of the anatase surface and by the strong hydrogen bond of adsorbates with the surface. In addition, the structure differences at 1/4 and 4/16 ML coverage revealed that a small cell fails to reproduce the surface relaxation. We also performed ab initio molecular dynamics simulations at 300 and 400 K. Complete cleavage and chemisorption structures are not stable at 8/16 ML coverage. They convert spontaneously to form a chemisorption and cleavage mixture. The chemisorption structure at full coverage is also unstable at room temperature. Moreover, the final structure depends on temperature, unlike at lower coverage. Our calculations challenge the traditional theory of chemical bonds because the strong hydrogen bond effects cause chemical

bond breaking. More experiments and theoretical researches are needed to gain a clear idea of the peculiar properties of adsorption on this type of surface.

ACKNOWLEDGMENTS

This work was supported by a grant from the Research Grants Council of the Hong Kong SAR (Project No. 11306219). This work was carried out using the computational facilities, CityU Burgundy, managed and provided by the Computing Services Centre at City University of Hong Kong (https://www.cityu.edu.hk/).

CONFLICT OF INTEREST

The authors declared that they have no conflicts of interest in this work.

REFERENCES

[1] K.W. Ting, T. Toyao, S.H. Siddiki, K.-i. Shimizu, Low-temperature hydrogenation of CO_2 to methanol over heterogeneous TiO_2-Supported Re catalysts, ACS Catal., 9 (2019), pp. 3685-3693.

[2] T. An, H. Yang, W. Song, G. Li, H. Luo, W.J. Cooper, Mechanistic considerations for the advanced oxidation treatment of fluoroquinolone pharmaceutical compounds using TiO_2 heterogeneous catalysis, J. Phys. Chem. A, 114 (2010), pp. 2569-2575.

[3] K.V. Kovtunov, D.A. Barskiy, A.M. Coffey, M.L. Truong, O.G. Salnikov, A.K. Khudorozhkov, E.A. Inozemtseva, I.P. Prosvirin, V.I. Bukhtiyarov, K.W. Waddell, High-Resolution 3D Proton MRI of Hyperpolarized Gas Enabled by Parahydrogen and Rh/TiO_2 Heterogeneous Catalyst, Chem. Eur. J., 20 (2014), pp. 11636-11639.

[4] Q. Sun, S. Wu, K. Li, B. Han, Y. Chen, B. Pang, L. Yu, L. Dong, The favourable synergistic operation of photocatalysis and catalytic oxygen reduction reaction by a novel heterogeneous $CoFe_2O_4$-TiO_2 nanocomposite, Appl. Surf. Sci., (2020), pp. 146142.

[5] H. Liu, Y. Feng, J. Shao, Y. Chen, Z.L. Wang, H. Li, X. Chen, Z. Bian, Self-cleaning triboelectric nanogenerator based on TiO_2 photocatalysis, Nano Energy, 70 (2020), pp. 104499.

[6] T. Paul, P.L. Miller, T.J. Strathmann, Visible-light-mediated TiO_2 photocatalysis of fluoroquinolone antibacterial agents, Environ. Sci. Technol., 41 (2007), pp. 4720-4727.

[7] P.A. Pekakis, N.P. Xekoukoulotakis, D. Mantzavinos, Treatment of textile dyehouse wastewater by TiO_2 photocatalysis, Water Res., 40 (2006), pp. 1276-1286.

[8] L. Yang, E.Y. Liya, M.B. Ray, Degradation of paracetamol in aqueous solutions by TiO_2 photocatalysis, Water Res., 42 (2008), pp. 3480-3488.

[9] J.H. Braun, A. Baidins, R.E. Marganski, TiO_2 pigment technology: a review, Prog. Org. Coat., 20 (1992), pp. 105-138.

[10] T. Thongkanluang, T. Kittiauchawal, P. Limsuwan, Preparation and characterization of Cr_2O_3–TiO_2–Al_2O_3–V_2O_5 green pigment, Ceram. Int., 37 (2011), pp. 543-548.

[11] C. Tian, S. Huang, Y. Yang, Anatase TiO_2 white pigment production from unenriched industrial titanyl sulfate solution via short sulfate process, Dyes Pigm., 96 (2013), pp. 609-613.

[12] M. Tian, Y. Liu, W. Wang, W. Zhao, D. Chen, L. Wang, H. Zhao, F. Meng, Y. Zhen, Z. Hu, Mechanism of synthesis of anatase TiO_2 pigment from low concentration of titanyl sulfuric–chloric acid solution under hydrothermal hydrolysis, J. Chin. Chem. Soc., 67 (2020), pp. 277-287.

[13] V. Galstyan, A. Ponzoni, I. Kholmanov, M.M. Natile, E. Comini, G. Sberveglieri, Highly sensitive and selective detection of dimethylamine through Nb-doping of TiO_2 nanotubes for potential use in seafood quality control, Sens. Actuators B Chem., 303 (2020), pp. 127217.

[14] C. Garzella, E. Comini, E. Tempesti, C. Frigeri, G. Sberveglieri, TiO_2 thin films by a novel sol–gel processing for gas sensor applications, Sens. Actuators B Chem., 68 (2000), pp. 189-196.

[15] B. Karunagaran, P. Uthirakumar, S. Chung, S. Velumani, E.-K. Suh, TiO_2 thin film gas sensor for monitoring ammonia, Mater. Charact., 58 (2007), pp. 680-684.

[16] A.M. Ruiz, G. Sakai, A. Cornet, K. Shimanoe, J.R. Morante, N. Yamazoe, Cr-doped TiO_2 gas sensor for exhaust NO_2 monitoring, Sens. Actuators B Chem., 93 (2003), pp. 509-518.

[17] Y. You, W. Tian, L. Min, F. Cao, K. Deng, L. Li, TiO_2/WO_3 bilayer as electron transport layer for efficient planar perovskite solar cell with efficiency exceeding 20%, Adv. Mater. Interfaces, 7 (2020), pp. 1901406.

[18] K. Hara, K. Sayama, Y. Ohga, A. Shinpo, S. Suga, H. Arakawa, A coumarin-derivative dye sensitized nanocrystalline TiO_2 solar cell having a high solar-energy conversion efficiency up to 5.6%, Chem. Commun., (2001), pp. 569-570.

[19] K. Murakoshi, R. Kogure, Y. Wada, S. Yanagida, Solid state dye-sensitized TiO_2

solar cell with polypyrrole as hole transport layer, Chem. Lett., 26 (1997), pp. 471-472.

[20] H.-S. Kim, J.-W. Lee, N. Yantara, P.P. Boix, S.A. Kulkarni, S. Mhaisalkar, M. Grätzel, N.-G. Park, High efficiency solid-state sensitized solar cell-based on submicrometer rutile TiO_2 nanorod and $CH_3NH_3PbI_3$ perovskite sensitizer, Nano Lett., 13 (2013), pp. 2412-2417.

[21] D. Zhang, G. Li, X. Yang, C.Y. Jimmy, A micrometer-size TiO_2 single-crystal photocatalyst with remarkable 80% level of reactive facets, Chem. Commun., (2009), pp. 4381-4383.

[22] S. Liu, J. Yu, M. Jaroniec, Tunable photocatalytic selectivity of hollow TiO_2 microspheres composed of anatase polyhedra with exposed {001} facets, J. Am. Chem. Soc., 132 (2010), pp. 11914-11916.

[23] X. Han, Q. Kuang, M. Jin, Z. Xie, L. Zheng, Synthesis of titania nanosheets with a high percentage of exposed (001) facets and related photocatalytic properties, J. Am. Chem. Soc., 131 (2009), pp. 3152-3153.

[24] H.G. Yang, C.H. Sun, S.Z. Qiao, J. Zou, G. Liu, S.C. Smith, H.M. Cheng, G.Q. Lu, Anatase TiO_2 single crystals with a large percentage of reactive facets, Nature, 453 (2008), pp. 638-641.

[25] X.-Q. Gong, A. Selloni, Reactivity of anatase TiO_2 nanoparticles: the role of the minority (001) surface, J. Phys. Chem. B, 109 (2005), pp. 19560-19562.

[26] A. Vittadini, A. Selloni, F. Rotzinger, M. Grätzel, Structure and energetics of water adsorbed at TiO_2 anatase (101) and (001) surfaces, Phys. Rev. Lett., 81 (1998), pp. 2954.

[27] A. Hussain, J. Gracia, B.E. Nieuwenhuys, J.H. Niemantsverdriet, Chemistry of O- and H-containing species on the (001) surface of anatase TiO_2: a DFT study, ChemPhysChem, 11 (2010), pp. 2375-2382.

[28] M. Kunat, U. Burghaus, C. Wöll, The adsorption of hydrogen on the rutile TiO_2(110) surface, Phys. Chem. Chem. Phys., 6 (2004), pp. 4203-4207.

[29] Y. Gui, W. Li, X. He, Z. Ding, C. Tang, L. Xu, Adsorption properties of pristine and Co-doped TiO_2 (1 0 1) toward dissolved gas analysis in transformer oil, Appl. Surf. Sci., 507 (2020), pp. 145163.

[30] A. Mahmood, G. Shi, X. Xie, J. Sun, Adsorption mechanism of typical oxygen, sulfur, and chlorine containing VOCs on TiO_2 (0 0 1) surface: First principle calculations, Appl. Surf. Sci., 471 (2019), pp. 222-230.

[31] L. Wang, Q. Wang, F. Ren, Y. Wang, An unexpected interaction between a H_2O_2 molecule and anatase TiO_2 (101) surface, Appl. Surf. Sci., 493 (2019), pp. 926-932.

[32] L. Lin, Z. Shi, J. Huang, P. Wang, W. Yu, C. He, Z. Zhang, Molecular adsorption properties of CH_4 with noble metals doped onto oxygen vacancy defect of anatase TiO_2 (1 0 1) surface: First-principles calculations, Appl. Surf. Sci., (2020), pp. 145900.

[33] A. Mahmood, G. Shi, X. Xie, J. Sun, Assessing the adsorption and photocatalytic activity of TiO_2 nanoparticles for the gas phase acetaldehyde: A computational and experimental study, J. Alloys Compd., 819 (2020), pp. 153055.

[34] Y. Zhang, W. Zeng, Y. Li, Computational study of surface orientation effect of rutile TiO_2 on H_2S and CO sensing mechanism, Appl. Surf. Sci., 495 (2019), pp. 143619.

[35] X.-Q. Gong, A. Selloni, A. Vittadini, Density functional theory study of formic acid adsorption on anatase TiO_2 (001): geometries, energetics, and effects of coverage, hydration, and reconstruction, J. Phys. Chem. B, 110 (2006), pp. 2804-2811.

[36] R. Tonner, Adsorption of proline and glycine on the TiO_2 (110) surface: a density functional theory study, ChemPhysChem, 11 (2010), pp. 1053-1061.

[37] A.M. Márquez, J.J. Plata, J.F. Sanz, Role of coverage and surface oxidation degree in the adsorption of acetone on TiO_2 (110). A density functional study, J. Phys. Chem. C, 113 (2009), pp. 19973-19980.

[38] H. Feng, S. Tan, H. Tang, Q. Zheng, Y. Shi, X. Cui, X. Shao, A. Zhao, J. Zhao, B. Wang, Temperature-and coverage-dependent kinetics of photocatalytic reaction of methanol on TiO_2 (110)-(1 × 1) surface, J. Phys. Chem. C, 120 (2016), pp. 5503-5514.

[39] F. Xu, X. Chen, W. Yang, X. Wang, X. Yang, Q. Guo, Coverage-Dependent

Ethylene Glycol Photochemistry on Rutile-TiO_2 (110), J. Phys. Chem. C, 124 (2020), pp. 14632-14639.

[40] B. Kim, Z. Li, B.D. Kay, Z. Dohnálek, Y.K. Kim, The effect of oxygen vacancies on the binding interactions of NH_3 with rutile TiO_2 (110)-1 × 1, Phys. Chem. Chem. Phys., 14 (2012), pp. 15060-15065.

[41] X.-j. Guo, W. Liu, W. Fang, L. Cai, Y. Zhu, L. Lu, X. Lu, DFT study of coverage-depended adsorption of NH_3 on TiO_2-B (100) surface, Phys. Chem. Chem. Phys., 14 (2012), pp. 16618-16625.

[42] P. McGill, H. Idriss, Ab Initio Study of Surface Acid− Base Reactions. The Case of Molecular and Dissociative Adsorption of Ammonia on the (011) Surface of Rutile TiO_2, Langmuir, 24 (2008), pp. 97-104.

[43] S. Selçuk, A. Selloni, Surface Structure and Reactivity of Anatase TiO_2 Crystals with Dominant {001} Facets, J. Phys. Chem. C, 117 (2013), pp. 6358-6362.

[44] I. Beinik, A. Bruix, Z. Li, K.C. Adamsen, S. Koust, B. Hammer, S. Wendt, J.V. Lauritsen, Water Dissociation and Hydroxyl Ordering on Anatase TiO_2(001)−(1 × 4), Phys. Rev. Lett., 121 (2018), pp. 206003.

[45] I. Katsounaros, M.C. Figueiredo, X. Chen, F. Calle-Vallejo, M.T. Koper, Structure- and Coverage-Sensitive Mechanism of NO Reduction on Platinum Electrodes, ACS Catal., 7 (2017), pp. 4660-4667.

[46] A. Markovits, J. Ahdjoudj, C. Minot, A theoretical analysis of NH_3 adsorption on TiO_2, Surf. Sci., 365 (1996), pp. 649-661.

[47] S. Yamazoe, T. Okumura, K. Teramura, T. Tanaka, Development of the efficient TiO_2 photocatalyst in photoassisted selective catalytic reduction of NO with NH_3, Catal. Today, 111 (2006), pp. 266-270.

[48] S. Yamazoe, T. Okumura, T. Tanaka, Photo-oxidation of NH_3 over various TiO_2, Catal. Today, 120 (2007), pp. 220-225.

[49] B. Dereka, Q. Yu, N.H. Lewis, W.B. Carpenter, J.M. Bowman, A. Tokmakoff, Crossover from hydrogen to chemical bonding, Science, 371 (2021), pp. 160-164.

[50] M. Bonn, J. Hunger, Between a hydrogen and a covalent bond, Science, 371 (2021), pp. 123-124.

[51] G. Kresse, J. Hafner, Ab initio molecular-dynamics simulation of the liquid-metal–amorphous-semiconductor transition in germanium, Phys. Rev. B, 49 (1994), pp. 14251.

[52] G. Kresse, J. Hafner, Ab initio molecular dynamics for liquid metals, Phys. Rev. B, 47 (1993), pp. 558.

[53] G. Kresse, J. Furthmüller, Efficiency of ab-initio total energy calculations for metals and semiconductors using a plane-wave basis set, Comput. Mater. Sci., 6 (1996), pp. 15-50.

[54] G. Kresse, D. Joubert, From ultrasoft pseudopotentials to the projector augmented-wave method, Phys. Rev. B, 59 (1999), pp. 1758.

[55] J.P. Perdew, K. Burke, M. Ernzerhof, Generalized gradient approximation made simple, Phys. Rev. Lett., 77 (1996), pp. 3865.

[56] S. Grimme, J. Antony, S. Ehrlich, H. Krieg, A consistent and accurate ab initio parametrization of density functional dispersion correction (DFT-D) for the 94 elements H-Pu, J. Chem. Phys., 132 (2010), pp. 154104.

[57] J. Neugebauer, M. Scheffler, Adsorbate-substrate and adsorbate-adsorbate interactions of Na and K adlayers on Al(111), Phys. Rev. B, 46 (1992), pp. 16067.

[58] S. Nosé, A unified formulation of the constant temperature molecular dynamics methods, J. Chem. Phys., 81 (1984), pp. 511-519.

[59] W.G. Hoover, Canonical dynamics: Equilibrium phase-space distributions, Phys. Rev. A, 31 (1985), pp. 1695.

[60] A. Ignatchenko, D.G. Nealon, R. Dushane, K. Humphries, Interaction of water with titania and zirconia surfaces, J. Mol. Catal. A-Chem., 256 (2006), pp. 57-74.

[61] A. Markovits, A. Fahmi, C. Minot, A theoretical study of CO_2 adsorption on TiO_2, J. Mol. Struct. THEOCHEM, 371 (1996), pp. 219-235.

[62] D. Sprinceana, M. Caldararu, N. Ionescu, A. Auroux, Calorimetric study of the

acidity and interface effects of tin dioxide layers deposited on another metal oxide, J. Therm. Anal. Calorim., 56 (1999), pp. 109-115.

[63] R. Erdogan, O. Ozbek, I. Onal, A periodic DFT study of water and ammonia adsorption on anatase TiO_2 (001) slab, Surf. Sci., 604 (2010), pp. 1029-1033.

[64] I. Onal, S. Soyer, S. Senkan, Adsorption of water and ammonia on TiO_2-anatase cluster models, Surf. Sci., 600 (2006), pp. 2457-2469.

[65] R. Erdogan, I. Onal, An ONIOM and DFT study of water and ammonia adsorption on anatase TiO_2 (001) cluster, Int. J. Quant. Chem., 111 (2011), pp. 2149-2159.

[66] E. Roman, J. De Segovia, Adsorption of ammonia on TiO_2(001) at room temperature, Surf. Sci., 251 (1991), pp. 742-746.

[67] T. Srnak, J. Dumesic, B. Clausen, E. Törnqvist, N.-Y. Topsøet, Temperature-programmed desorption/reaction and in situ spectroscopic studies of vanadia/titania for catalytic reduction of nitric oxide, J. Catal., 135 (1992), pp. 246-262.

[68] K.R. Hahn, A. Tricoli, G. Santarossa, A. Vargas, A. Baiker, First principles analysis of H_2O adsorption on the (110) surfaces of SnO_2, TiO_2 and their solid solutions, Langmuir, 28 (2012), pp. 1646-1656.

[69] E. Hyde, M. Beck, Comprehensive DFT study of hydroxyl coverage on titania surfaces, Appl. Surf. Sci., 498 (2019), pp. 143893.

[70] J. Ahdjoudj, A. Markovits, C. Minot, Hartree–Fock periodic study of the chemisorption of small molecules on TiO_2 and MgO surfaces, Catal. Today, 50 (1999), pp. 541-551.

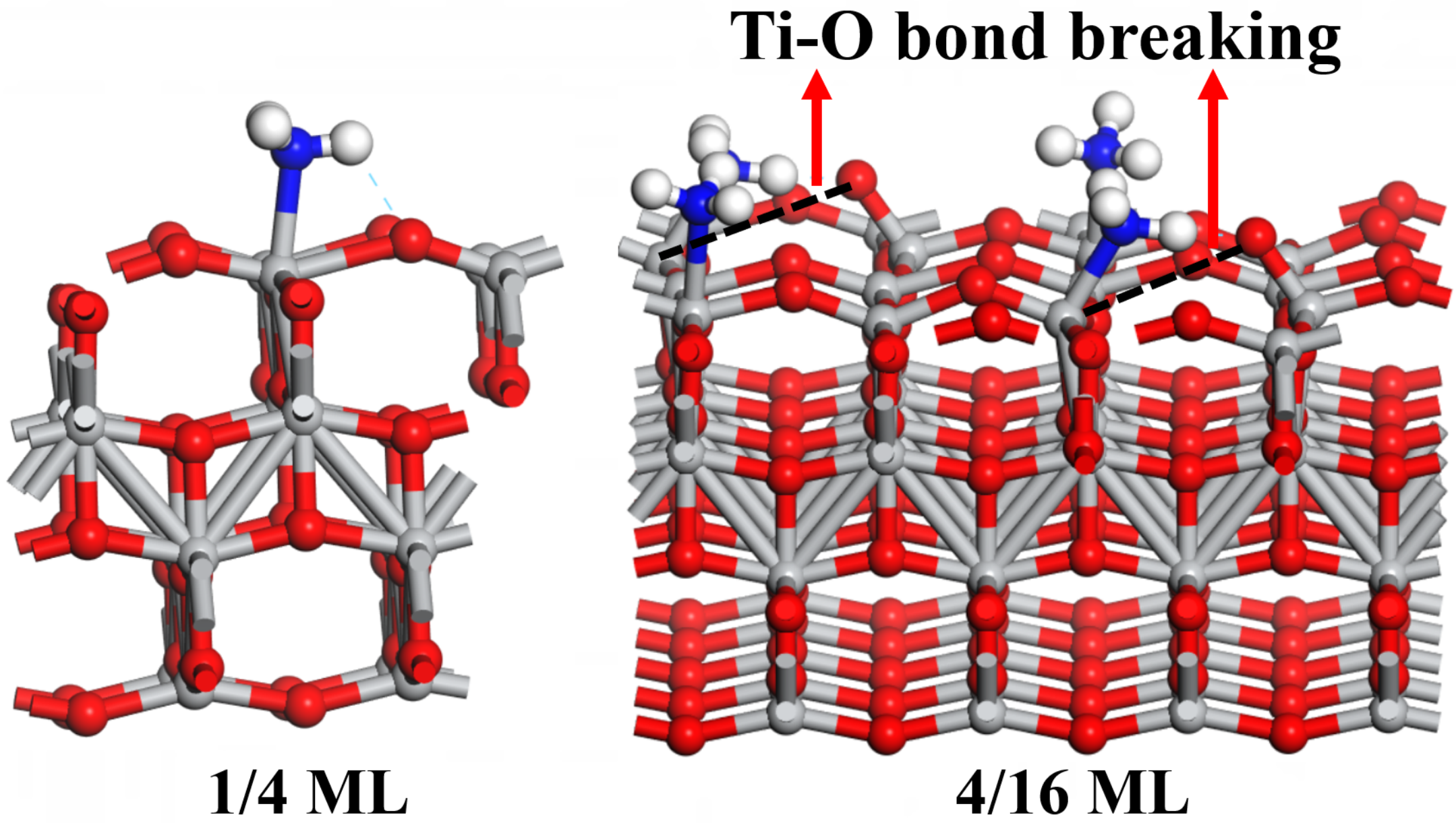
Ti-O bond breaking
1/4 ML
4/16 ML